Visual Neuroscience (2008), **25**, 215–220. Printed in the USA.

doi: 10.1017/S0952523808080498

BRIEF COMMUNICATION

Retinal ganglion cell density of the black rhinoceros (*Diceros bicornis*): Calculating visual resolution

JOHN D. PETTIGREW[1] AND PAUL R. MANGER[2]

[1]Queensland Brain Institute, University of Queensland, Australia
[2]School of Anatomical Sciences, University of the Witwatersrand, Johannesburg, Republic of South Africa

(RECEIVED January 10, 2008; ACCEPTED February 25, 2008)

Abstract

A single right retina from a black rhinoceros was whole mounted, stained and analyzed to determine the visual resolution of the rhinoceros, an animal with reputedly poor eyesight. A range of small (15-μm diameter) to large (100-μm diameter) ganglion cell types was seen across the retina. We observed two regions of high density of retinal ganglion cells at either end of a long, but thin, horizontal streak. The temporal specialization, which receives light from the anterior visual field, exhibited a ganglion cell density of approximately 2000/mm^2, while the nasal specialization exhibited a density of approximately 1500/mm^2. The retina exhibited a ganglion cell density bias toward the upper half, especially so, the upper temporal quadrant, indicating that the rhinoceros would be processing visual information from the visual field below the anterior horizon for the most part. Our calculations indicate that the rhinoceros has a visual resolution of 6 cycles/degree. While this resolution is one-tenth that of humans (60 cycles/deg) and less than that of the domestic cat (9 cycles/deg), it is comparable to that of the rabbit (6 cycles/deg), and exceeds that seen in a variety of other mammals including seals, dolphins, microbats, and rats. Thus, the reputation of the rhinoceros as a myopic, weakly visual animal is not supported by our observations of the retina. We calculate that the black rhinoceros could readily distinguish a 30 cm wide human at a distance of around 200 m given the appropriate visual background.

Keywords: Retina, Whole mount, Area centralis, Perissodactyl, Mammal, Ganglion cell layer

Introduction

The black rhinoceros is one of the most well known creatures on the African continent, but due to relentless poaching and human usurpation of its primary habitat, its numbers have dwindled to the level where this mammal appears on the International Union for Conservation of Nature (IUCN) red list as critically endangered (www.iucn.org/themes/ssc/redlist.html). The family Rhinocerotidae are part of the order Perissodactyla (which includes horses, zebras, donkey, and tapirs) and is comprised of five extant species (Nowak, 1999). All species of rhinoceros are thought to have poor eyesight based on observations of both the anatomy of the eye and naturalists' reports (Thomas, 1801; Skinner & Chimimba, 2005; see also Fig. 12 in Hughes, 1977). The black rhinoceros is reported to be uninterested in a stationary person or vehicle unless that person or vehicle is closer than 20–30 m (Nowak, 1999), while white rhinoceroses have been reported to discern moving objects at up to 40 m (Skinner & Chimimba, 2005). Rhinoceroses are often considered to be myopic (or near-sighted), but an examination of the refractive state of the eyes of white and black rhinoceroses indicated them to be mildly hyperopic (or far-sighted) (Howland et al., 1993).

Rhinoceroses are thought to rely upon olfaction and audition for the majority of their sensory discrimination (Skinner & Chimimba, 2005), with white rhinoceros reportedly detecting human scent from up to 800 m when downwind (Owen-Smith, 1973); however, some observations do indicate that the visual resolution and ability of the rhinoceroses may have been underestimated, as the black rhinoceros may initiate a charge from up to 70 m distance (Skinner & Chimimba, 2005). Daniel (1994) has demonstrated that the white rhinoceros (*Ceratotherium simum*) was able to see and respond to a life-size image of another rhinoceros at a distance of around 30 m. A second study demonstrated that two white rhinoceroses could learn to visually discriminate between a circle (35.5 cm outer diameter, 15 cm inner diameter, black on white background) and an isosceles triangle (40.6 cm sides, 5 cm thick black lines on white background) placed 4.6 m apart at distances of between 4 to 10 m (Daniel & Mikulka, 1998). In the same study, after mastery of the visual discrimination task, one rhinoceros was tested on discriminating between an open (35.5 cm outer diameter, 15 cm inner diameter, black on white background) and a closed (35.5 cm

Address correspondence and reprint requests to: Paul Manger, School of Anatomical Sciences, Faculty of Health Sciences, University of the Witwatersrand, 7 York Road, Parktown, 2193, Johannesburg, Republic of South Africa. E-mail: paul.manger@wits.ac.za

outer diameter, black on white background) circle under similar conditions; however, the rhinoceros failed to perform above chance in this task (Daniel & Mikulka, 1998). This latter task would appear to indicate that the visual resolution of the rhinoceros is poor, not being able to discriminate an image around 15 cm in diameter from a distance of 4 m or more; however, Daniel and Mikulka (1998) do point out that the animal tested may not have been paying attention to the salient feature of the signal in this task.

To date the visual resolution of any rhinoceros species has not been determined. Since retinal ganglion cell density combined with eye size can be used to determine visual resolution, this method has been used in many species to predict the limits of visual ability (e.g., Hughes, 1975, 1977; Pettigrew et al., 1988). We were fortunate enough to obtain a single right eye from a black rhinoceros that was being euthanazed for veterinary reasons and were able to calculate an estimate of the visual resolution of the black rhinoceros from this one specimen.

Materials and methods

A single adult male black rhinoceros (*Diceros bicornis*) was humanely euthanazed because of an intractable gastrointestinal illness and severe chronic otitis externa. This approximately 40 year-old animal was under the care of the National Zoological Gardens of South Africa, the veterinarians of which made all decisions concerning the well being and euthanasia of this animal. During euthanasia, the eye was covered with a dark cloth in an attempt to dark-adapt the eye to reduce adherence of the pigment epithelium to the retina. Following cardiac arrest, the head and neck was dissected free from the body and perfused using a gravity feed *via* paired carotid arteries, initially with a 20 l rinse of 0.9% saline to flush the remaining blood followed by 40 l of fixative (4% paraformaldehyde in 0.1 M phosphate buffer). The right eye was removed immediately after perfusion, a large slit was cut at the junction of the anterior and posterior chambers, and the vitreous humor removed with gentle pressure. The eye was then immerse-fixed in a solution containing 2% paraformaldehyde, 0.1M L-lysine and 0.01M sodium m-periodate in 0.5M phosphate buffer for 2 h at 4°C (McLean & Nakane, 1974). After this, the eye was placed in 0.1 M phosphate buffer containing 0.05% sodium azide and stored at 4°C. The left eye of this animal had been lost during an altercation with another black rhinoceros five years previously.

The retina was dissected from the remainder of the eye under a dissecting microscope and placed on a large gelatine coated glass slide. Strategic cuts were made in the retina to allow it to be flattened and adhere to the slide. After partially drying and adhering to the glass, a solution of 0.1% cresyl violet was dripped over the retina to stain the ganglion cells. The stain was then differentiated with acetic acid and 70% ethanol to ensure staining of only the ganglion cell layer. The slide with the retina was then passed through a series of graded alcohols, cleared in xylene and coverslipped using Depex mounting medium.

The retina was drawn on a sheet of A3 graph paper (2 mm grid) using an overhead projector at a magnification of 4×. Care was taken to align the side of the microscope slide to the graph paper grid so the movements of the stage micrometer would be parallel to the grid. The X-Y coordinates of a number of landmarks on the retina were noted on the drawing so that all subsequent counts could be transferred to the drawing from the stage micrometer. A 10×10 square eyepiece graticule, subtending 200 micra on a side, was used to count ganglion cells. The large, Nissl-filled retinal ganglion neurons in this species were relatively easy to distinguish from the much smaller nuclei and absent Nissl substance of glia and displaced amacrine cells (Fig. 1). The inclusion/exclusion of displaced amacrine cells is a controversial issue in counts of retinal whole mounts (e.g., Stone (1983) and Hughes (1977) had a long interaction over this issue). In the present case, the distinction between retinal ganglion cells and displaced amacrines was stark, because of the large size of the ganglion cells, their multipolar shape, prominent nucleolus and dense Nissl substance compared with the ovoid nuclei and lack of a prominent nucleolus and indistinct cytoplasm of the much smaller displaced amacrine cells (Fig. 1). Because counts of density from the ganglion cell layer are reduced to the square root for the purposes of resolution estimations, the ganglion cell/amacrine boundary distinction is not a major issue, even in the presence of an error. In the Stone-Hughes controversy about the number of retinal ganglion cells in the cat,

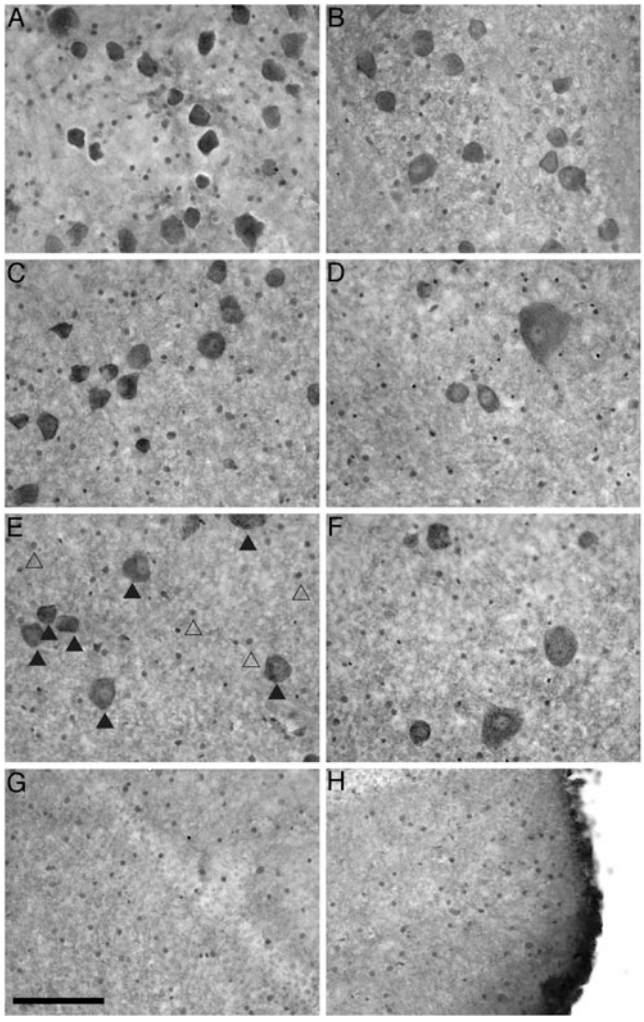

Fig. 1. Photomicrographs of Nissl stained retinal ganglion cell bodies in the whole mounted retina of the black rhinoceros. **A** is taken from the region of highest density, with progressive photomicrographs taken every few millimetres through to the edge of the retina (**H**). Note the range of sizes and types of ganglion cells. The smaller displaced amacrine and glial cell bodies are also visible. Examples of retinal ganglion cells (solid arrowheads) and displaced amacrine cells (open arrowheads) are shown in **E** and indicate the dramatic difference in size of these two cells types in the retina of the rhinoceros. Scale bar in **G** = 100 μm and applies to all.

the range of estimates varied from 90,00 to 220,000, a seemingly large margin of error for this estimate, but one which leads to a range of 300–469 for the linear estimate of cell numbers used to calculate resolution. In this example, a large overestimate as a result of including too may displaced amacrines would result in only a 23% overestimate of resolution, an insignificant error compared with the two orders of magnitude interspecific variation in mammalian acuity (Table 1). Variation in displaced amacrine cell estimates becomes more significant in the periphery, where the retinal ganglion cell density falls off much more than the displaced amacrine cell density. This results in an attenuation of the centro-peripheral gradient if one errs on the side of including more displaced amacrine cells. The centro-peripheral gradient is not a central issue in this paper, whose aim is to help clarify the poor current picture of the rhino's retinal ganglion cell resolution without making any pretensions about more subtle issues of retinal ganglion cell-layer anatomy that might require retrograde transport techniques not available in the limited circumstances of the present study. Nevertheless, we do not think that we have made a large number of errors in distinguishing retinal ganglion cells from displaced amacrine cells, for the reasons already given.

Counts in the 100 squares of the graticule (40,000 sq. micra) were divided by 0.4 to give density in cells/mm^2, which were then transferred to the map. Counts were obtained every 2–4 mm, with gaps at some places, such as near the optic nerve head or at blemishes. Contour lines of isodensity were drawn and smoothed by manual interpolation. We estimated that this rhino eye was 0.28 mm/deg, using the A-P distance of the eye 0.6× (Pettigrew et al., 1988) and the estimate that the horizontal dimension of the eye, corresponding to ~180° was ~50 mm. From the maximum density estimates, 2000 cells/mm^2, as well as the retinal magnification factor of 0.28 mm/deg, one can calculate that there are 45 (square root of 2000) cells per mm. According to the Nyquist limit, one needs twice the resolution to achieve the outcome, so there are 23 cells/mm contributing to the rhinoceros's visual resolution. Using the value of 0.28 mm/deg, we get 6 cycles/deg (23 × 0.28 cycles/deg).

Digital photomicrographs were captured using a Zeiss Axioskop and the Axiovision software. No adjustments of pixels, or manipulation of the captured images were undertaken, except for the adjustment of contrast, brightness, and levels using Adobe Photoshop 7.

Results

Retinal ganglion cells

Retinal ganglion cells were noteworthy for the range of sizes, with the largest being more than 100 μm across while the smallest were around 15 μm (Fig. 1). Despite the large size range, the intense Nissl substance in the cytoplasm and the prominent nucleus and nucleolus made the retinal ganglion cells easy to distinguish from the much smaller displaced amacrine cells (ovoid granular nuclei < 10 μm and no visible Nissl substance) and glial nuclei (uniformly dark nuclei ~5 μm) (see Fig. 1E).

Topography

There was an area centralis in the temporal retina where the ganglion cell density peaked at 2000 cells/mm^2, giving a predicted visual resolution of 6 cycles/degree (see calculation provided in

Table 1. *Comparative visual acuity calculations. Where possible, the Table includes for each species, both visual acuity estimated from eye size and retina ganglion cell density and grating visual acuity determined behaviourally. After each taxon the letters in parentheses indicate its affinities: (A) Aves; (Pr) Primates; (Pe) Perissodactyls; (Ca) Carnivores; (R) Rodents; (Ma) Marsupials; (O) Odontocetes; (L) Lagomorphs; (Ce) Cephalopods; (Mi) Microbats*

Species	Visual resolution (cycles/deg) calculated from retina	Reference (retina)	Behavioral measure of visual acuity (cycles/deg)	Reference (behav.)
Eagle (A)	147	Reymond, 1985	140	Reymond, 1985
Human (Pr)	65	Curcio & Allen, 1990	60	Campbell & Gubisch, 1967
Horse (Pe)	25	Evans & McGreevy, 2007	20	Timney & Keil, 1992
Pigeon (A)	18	Remy & Gunturkun, 1991	12	Hodos et al., 1976
Cat (Ca)	10	Cleland et al., 1982	9	Hall & Mitchell, 1991
Hyena (Ca)	8.4	Calderone et al., 2003	—	—
Agouti (R)	7	Silveira et al., 1989	—	—
Harp seal (Ca)	—	—	6.8	Mass & Supin, 2003
Numbat (Ma)	6.3	Arrese et al., 2000	5.2	Arrese et al., 2000
Dolphin (O)	6	Mass & Supin, 1995	3	Pepper & Simmons, 1973
Tammar wallaby (Ma)	6	Hemmi & Mark, 1998	4.8	Hemmi & Mark, 1998
Rhinoceros (Pe)	6	This study	—	—
Rabbit (L)	6	Vaney & Hughes, 1976	—	—
Capybara (R)	6	Silveira et al., 1989	—	—
Harbour seal (Ca)	5	Weiffen et al., 1992	—	—
Octopus (Ce)	—	—	4	Muntz & Gwyther, 1989
Paca (R)	3	Silveira et al., 1989	—	
Native cat (Ma)	3	Harman et al., 1986	3	Harman et al., 1986
Ghost bat (Mi)	2	Pettigrew et al., 1988	—	—
Rat (R)	1	Dean, 1981	1	Prusky et al., 2000
Little brown bat (Mi)	0.8	Koay et al., 1998	0.5	Bell & Fenton, 1986
Mouse (R)	0.6	Gianfranceschi et al., 1999	0.6	Gianfranceschi et al., 1999

Materials and methods). There was a prominent, but very narrow, horizontal retinal streak at around 600 cells/mm^2 (Fig. 2). Surprisingly, there was a second area centralis at the nasal end of the streak where cell density peaked at 1500 cells/mm^2, giving a predicted visual resolution posteriorly of 5 cycles/deg, close to the anterior peak resolution of 6 cycles/deg.

Isodensity contours form an axe-shaped protuberance above the temporal end of the horizontal streak and the temporal area centralis, representing the visual field below the rhinoceros' horizon (Fig. 2). This echoes the fact that superior retina, above the streak, has a greater area than inferior retina, below the streak. This axe-shaped arrangement has been described previously in browsing mammals (e.g., Hebel, 1976). It is very likely that this specialization for the region between the horizon and the animal's feet is also concerned with browsing in the rhinoceros. That more retina is devoted to the upper retina (for the lower field below the horizon) than is devoted to lower retina that looks up, above the horizon, could also be connected to browsing (Fig. 2). This arrangement places more emphasis on the lower field between the horizon and the feet, as would be appropriate for a browser.

Optic nerve head

The optic disc is slightly elongated, which is not a common feature in a mammal. The axis through the ellipse is oriented at approximately 45° to the horizontal (as given by the horizontal retinal streak) (Fig. 2). This oblique orientation should be detectable ophthalmoscopically and thus provide the major horizontal axis of the retina in the living animal.

Discussion

Sample size

One would normally be hesitant about accepting data from a single eye, particularly when the animal had been put down for medical reasons. On the other hand, the opposite eye of this rhino had been lost because of trauma, not disease, and the retina we studied showed no sign of disease. The retinal ganglion cells were large and loaded with Nissl substance, along with prominent nucleoli, and showed no signs of degeneration. Since the large retinal neurons are the first to be compromised (Wang et al., 1996), the evident health of the rhino's very large ganglion cells argues strongly that this was a normal retina. It is also hard to imagine how pathology could have produced the smooth isodensity contours of the dual specialization that we have described. For these reasons, we think it important that we report this unusual retinal specialization, one that is unique to date in terrestrial mammals. One role of a larger sample is to cover the vagaries of dissection and the variable, problematical adherence of pigment epithelium that prevents a view of the ganglion cell layer. As we were lucky with the dissection, and since the lithium-periodate fixation that we used resulted in a pigment-free retina, a sample of one retina was sufficient for the present purposes. Finally, the endangered status of the black rhino means that opportunities to study its retina are unlikely to be a regular occurrence.

Vision of the rhinoceros

Speculation on the visual capabilities of the rhinoceros can be partly settled by our retinal ganglion cell density measurements. The optic nerve is a bottleneck, such that the axons of retinal ganglion cells are the only means by which the retina can pass visual information to other parts of the central nervous system. The visual behavior of the whole animal cannot therefore exceed what is provided to the brain by the retinal ganglion cells. Retinal ganglion cell density has thus been used to estimate the visual resolution of a wide variety of vertebrates, with excellent predictive value of ganglion cell measurement for the behavior of the whole animal (e.g., Hughes, 1975, 1977; Pettigrew et al., 1988). While the maximum retinal ganglion cell density we measured in the rhinoceros is modest, at only 2000 cells/mm^2, the large eye means that this translates to a visual resolution of 6 cycles/deg (see Materials and methods for calculation). This is one-tenth the visual resolution of humans, who have the highest visual resolution of any mammal (Curcio & Allen, 1990), and half the visual resolution of a domestic cat (Hughes, 1975). To put this into context, bearing in mind that one degree subtends approximately 200 cm at 100 m,

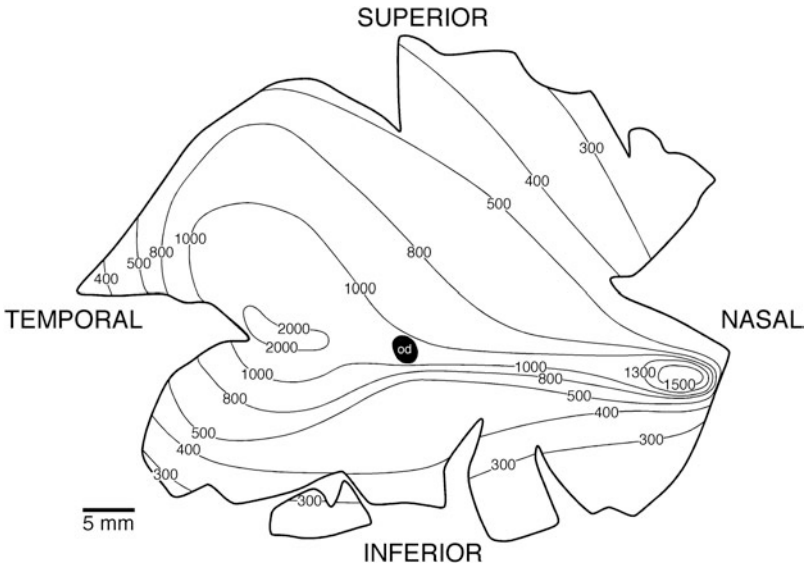

Fig. 2. Retinal topography of all cells within the ganglion cell layer stained with Nissl substance in the right eye of the black rhinoceros. Note the dual density specializations located at the temporal (2000 cells/mm^2) and nasal (1500 cells/mm^2) ends of the thin but prominent horizontal visual streak (1000 cells/mm^2). The optic disc (**od**) is slightly elongated and at an angle of around 45° to the horizontal streak.

this value would mean that the rhinoceros would be able to resolve a target that was 17 cm wide (200/12) against a background at a distance of 100 m. If the target were silhouetted against a bright sky, a considerably smaller width would be visible because of the line spread function. Based on the same measurement of 6 cycles/deg, a 30 cm wide human would be visible to the rhinoceros, against a background, at a distance of about 200 m. This value seems apposite in that one does seem to begin to excite a rhinoceros at that distance if moving (J.D. Pettigrew, personal observations), although other anecdotal reports suggest approximately half this distance (e.g., Skinner & Chimimba, 2005). Our measurements thus suggest a much more optimistic account of rhinoceros visual resolution compared with the values obtained by the behavioral tests of Daniel and Mikulka (1998), which may have lacked a means to attract the attention of their uncooperative subject. A refractive study indicated that the rhinoceros was slightly hyperopic when relaxed (Howland et al., 1993) not myopic as suggested by indirect measures (see Fig. 12 in Hughes, 1977). This ability to achieve a distant focus is in keeping with the prominent visual streak that one imagines would not be trained on the near field, but rather on the horizon at infinity, as the streak is disposed in other animals with this specialization (e.g., Silveira et al., 1989).

Comparison with other animals

We have provided Table 1 to show a range of visual acuities in a series of animals, where possible calculated from retinal ganglion cell numbers as well as from behavioral estimates. While the rhinoceros fails to match the visual resolution of many animals, the observed 6 cycles/deg is equal to the rabbit and exceeds that of murid rodents (1 cycle/deg), false vampire microbats or ghost bats (2 cycles/deg), bottlenose dolphins (3 cycles/deg), the octopus (4 cycles/deg), and the seal (5 cycles/deg).

The only other perissodactyl for which there is retinal whole mount data is the horse (Hebel, 1976). This original description and a more recent one (Guo & Sugita, 2000) do not indicate a dual specialization for the horse as seen in the rhinoceros, but a very recent study does indicate the potential of nasal and temporal specializations at either end of the horizontal streak although this has not been explicitly described (Evans & McGreevy, 2007). More detailed mapping of the retinal ganglion cell distribution in the horse is required to see if this dual specialization is a perissodactyl feature or specific to the rhinoceros. Behavioral data on visual resolution in the horse predicts that acuity is 23.3 cycles/deg (Timney & Keil, 1992). Estimates of the peak ganglion-cell density in the horse are approximately 6500 cells/mm^2 (Hebel, 1976). This calculates to be 24 cycles/deg of visual resolution (if one uses the posterior nodal distance of 35 mm, and the resulting 1.6 deg/mm provided by Coile & O'Keefe, 1988) and is very similar to that seen behaviorally. Thus, our calculations for the rhinoceros would appear to be a good prediction of its potential behavioral visual acuity. This excellent fit between visual resolution and behavioral visual acuity can be seen for most species (Table 1), where the retina ganglion cell estimate and the behavioral estimate are close, with the ganglion cell estimate slightly higher.

The rhinoceros has a ganglion cell density map that, in light of what is known to date, is unique in a terrestrial environment for mammals due to its dual specialization. A dual specialization of ganglion cell density in the nasal and temporal retina has been reported previously for the aquatic bottlenose dolphin (Mass & Supin, 1995). In the bottlenose dolphin, the ganglion cell density was around 670 cells/mm^2 providing a visual resolution of 3 cycles/deg in both specializations, which is around half that seen in the rhinoceros. Furthermore, the rhinoceros does not suffer from the quality of the marine medium diffusing and diffracting light, as does the dolphin. While dual specializations are well known for fish retinas and for the avian bifoveate retinas, which are found in all diurnal predatory birds (Collin, 2008), this is the first described case of two specializations in the retina of a terrestrial mammal. The two specializations occur at either end of the horizontal streak, so it might be considered that the nasal specialization is really just an extreme variation of the streak. On the other hand, the shape of the contours in this region indicate that it is a distinctive feature with a density that is 30% higher than the nearby regions of the streak and 400% greater than surrounding peripheral nasal retina.

The nasal area centralis would lie on the horizon of the rhinoceros but around 130° from straight ahead, as far in the posterior direction as the great bulk of this animal would perhaps allow it to see. Since predator species of rhinoceros are very few (possibly only lions and hyenas for subadults and calves respectively, Brain et al., 1999; plus fatal attacks by elephants, Slotow et al., 2001), and thus unlikely to explain the selective pressure that gave rise to this feature, perhaps the nasal, posterior-pointing area plays a role in conspecific encounters, during which there may be considerable danger if an adversary approached unheralded from the rear.

Acknowledgments

The authors would like to thank the members of the National Zoological Gardens of South Africa for allowing us to use this specimen for research. In particular, we thank Drs. Adrian Tordiffe and Ian Espie, and Prof. Antoinette Kotze for all their untiring assistance. We also thank Adhil Bhagwandin, Jason Hemingway, and Goran Strkalj for their enthusiastic assistance in the perfusion and subsequent fixation of the specimen used. The Department of Education South Africa research incentive scheme and the National Research Foundation of South Africa funded this work.

References

Arrese, C., Archer, M., Runham, P., Dunlop, S.A. & Beazley, L.D. (2000). Visual system in a diurnal marsupial, the numbat (*Myrmecobius fasciatus*): Retinal organization, visual acuity and visual fields. *Brain, Behavior and Evolution* **55**, 163–175.

Bell, G.P. & Fenton, M.B. (1986). Visual acuity, sensitivity and binocularity in a gleaning insectivorous bat, *Macrotus californicus* (Chiroptera, Phyllostomidae). *Animal Behavior* **34**, 409–414.

Brain, C., Forge, O. & Erb, P. (1999). Lion predation on black rhinoceros (*Diceros bicornis*) in Etosha National Park. *African Journal of Ecology* **37**, 107–109.

Calderone, J.B., Reese, B.E. & Jacobs, G.H. (2003). Topography of photoreceptors and retinal ganglion cells in the spotted hyena (*Crocuta crocuta*). *Brain, Behavior and Evolution* **62**, 182–192.

Campbell, F.W. & Gubisch, R.W. (1967). The effect of chromatic aberration on visual acuity. *Journal of Physiology* **192**, 345–358.

Cleland, B.G., Crewther, D.P., Crewther, S.G. & Mitchell, D.E. (1982). Normality of spatial resolution of retinal ganglion cells in cats with strabismic amblyopia. *Journal of Physiology* **326**, 235–249.

Coile, D.C. & O'Keefe, L.P. (1988). Schematic eyes for domestic animals. *Ophthalmic and Physiological Optics* **8**, 215–220.

Collin, S.P. (2008). A web-based archive for topographic maps of retinal cell distribution in vertebrates. *Clinical and Experimental Optometry* **91**, 85–95.

Curcio, C.A. & Allen, K.A. (1990). Topography of ganglion cells in human retina. *The Journal of Comparative Neurology* **300**, 5–25.

Daniel, J.C. (1994). Visual acuity of the rhinoceros. *AZA Annual Conference Proceedings*, pp. 343–346.

Daniel, J.C. & Mikulka, P.J. (1998). Discrimination learning in the white rhinoceros. *Applied Animal Behaviour Science* **58**, 197–202.

Dean, P. (1981). Visual pathways and acuity in hooded rats. *Behavioral Brain Research* **3**, 239–271.
Evans, K.E. & McGreevy, P.D. (2007). The distribution of ganglion cells in the equine retina and its relationship to skull morphology. *Anatomia, Histologica, Embryologia* **36**, 151–156.
Gianfranceschi, L., Fiorentini, A. & Maffei, L. (1999). Behavioural visual acuity of wild type and bcl2 transgenic mouse. *Vision Research* **39**, 569–574.
Guo, X. & Sugita, S. (2000). Topography of ganglion cells in the retina of the horse. *Journal of Veterinary Medical Science* **62**, 1145–1450.
Hall, S.E. & Mitchell, D.E. (1991). Grating acuity of cats measured with detection and discrimination tasks. *Behavioral Brain Research* **44**, 1–9.
Harman, A.M., Nelson, J.E., Crewther, S.G. & Crewther, D.P. (1986). Visual acuity of the northern native cat (*Dasyurus hallucatus*)—behavioural and anatomical estimates. *Behavioral Brain Research* **22**, 211–216.
Hebel, R. (1976). Distribution of retinal ganglion cells in five mammalian species (pig, sheep, ox, horse, dog). *Anatomy and Embryology* **150**, 45–51.
Hemmi, J.M. & Mark, R.F. (1998). Visual acuity, contrast sensitivity and retinal magnification in a marsupial, the tammar wallaby (*Macropus eugenii*). *Journal of Comparative Physiology A* **183**, 379–387.
Hodos, W., Leibowitz, R.W. & Bonbright, J.C. (1976). Near-field visual acuity of pigeons: Effects of head position and stimulus luminance. *Journal of the Experimental Analysis of Behavior* **25**, 129–141.
Howland, H.C., Howland, M. & Murphy, C.J. (1993). Refractive state of the rhinoceros. *Vision Research* **33**, 2649–2651.
Hughes, A. (1975). A quantitative analysis of the cat retinal ganglion cell topography. *The Journal of Comparative Neurology* **163**, 107–128.
Hughes, A. (1977). The topography of vision in mammals of contrasting lifestyles: comparative optics and retinal organization. In *Handbook of Sensory Physiology. Volume VII/5, The Visual System in Vertebrates*, ed. Crescitelli, F., pp. 613–756. New York: Springer-Verlag.
Koay, G., Kearns, D., Hefner, H.E. & Hefner, R.S. (1998). Passive sound-localization ability of the big brown bat (*Eptesicus fuscus*). *Hearing Research* **119**, 37–48
Mass, A.M. & Supin, A.Ya. (1995). Ganglion cell topography of the retina in the bottlenosed dolphin. *Brain, Behavior and Evolution* **45**, 257–265.
Mass, A.M. & Supin, A.Ya. (2003). Retinal topography of the harp seal, *Pagophilus groenlandicus*. *Brain, Behavior and Evolution* **62**, 212–222.
McLean, I.W. & Nakane, P.K. (1974). Periodate-lysine-paraformaldehyde fixative. A new fixation for immunoelectron microscopy. *Journal of Histochemistry and Cytochemistry* **22**, 1077–1083.
Muntz, W.R. & Gwyther, J. (1989). The visual acuity of octopuses for grating of different orientations. *Journal of Experimental Biology* **142**, 461–464.
Nowak, R.M. (1999). *Walker's Mammals of the World, 6th edition, Volume II*. Baltimore: The Johns Hopkins University Press.
Owen-Smith, N. (1973). The behavioural ecology of the white rhinoceros. Ph.D. Thesis, Madison: University of Wisconsin.
Pepper, R.L. & Simmons, J.V. (1973). In-air visual acuity of the bottlenose dolphin. *Experimental Neurology* **41**, 271–276.
Pettigrew, J.D., Dreher, B., Hopkins, C.S., McCall, M.J. & Brown, M. (1988). Peak density and distribution of ganglion cells in the retinae of microchiropteran bats: Implications for visual acuity. *Brain, Behavior and Evolution* **32**, 39–56.
Prusky, G.T., West, P.W. & Douglas, R.M. (2000). Experience-dependent plasticity of visual acuity in rats. *European Journal of Neuroscience* **12**, 3781–3786.
Remy, M. & Gunturkun, O. (1991). Retinal afferents to the tectum opticum and the nucleus opticus principalis thalami in the pigeon. *The Journal of Comparative Neurology* **305**, 57–70.
Reymond, L. (1985). Spatial visual acuity of the eagle *Aquila audax*: A behavioural, optical and anatomical investigation. *Vision Research* **25**, 1477–1491.
Silveira, L.C., Picanco-Diniz, C.W. & Oswaldo-Cruz, E. (1989). Distribution and size of ganglion cells in the retinae of large Amazonian rodents. *Visual Neuroscience* **2**, 221–235.
Skinner, J.D. & Chimimba, C.T. (2005). *The Mammals of the Southern African Subregion, 3rd Edition*. Cambridge, UK: Cambridge University Press.
Slotow, R., Balfour, D. & Howison, O. (2001). Killing of black and white rhinoceroses by African elephants in Hluhluwe-Umfolozi Park, South Africa. *Pachyderm* **31**, 14–20.
Stone, J. (1983). *The Classification of Retinal Ganglion Cells and its Impact on the Neurobiology of Vision*. New York: Plenum Press.
Thomas, H.L. (1801). An anatomical description of the male rhinoceros. *Philosophical Transactions of the Royal Society of London* **4**, 145–152.
Timney, B. & Keil, K. (1992). Visual acuity in the horse. *Vision Research* **32**, 2289–2293.
Vaney, D.I. & Hughes, A. (1976). The rabbit optic nerve: Fibre diameter spectrum, fibre count, and comparison with a retinal ganglion cell count. *The Journal of Comparative Neurology* **170**, 241–251.
Wang, C., Dreher, B. & Burke, W. (1996). Effects of eliminating retinal Y cell input on center-surround interactions in the dorsal lateral geniculate nucleus of the cat. *Visual Neuroscience* **13**, 1089–1097.
Weiffen, M., Möller, B., Mauck, B. & Dehnhardt, G. (1992). Effect of water turbidity on the visual acuity of harbor seals (*Phoca vitulina*). *Vision Research* **32**, 2289–2293.